Supramolecular Chemistry
Publication details, including instructions for authors and subscription information:
http://www.informaworld.com/smpp/title~content=t713649759

Inclusion of the allicin mimic *S-p*-tolyl *t*-butylthiosulphinate in β-cyclodextrin

Nashia Stellenboom[a]; Roger Hunter[a]; Mino R. Caira[a]; Susan A. Bourne[a]; Marco Barbieri[a]
[a] Department of Chemistry, University of Cape Town, Rondebosch, South Africa

To cite this Article Stellenboom, Nashia , Hunter, Roger , Caira, Mino R. , Bourne, Susan A. and Barbieri, Marco(2009) 'Inclusion of the allicin mimic *S-p*-tolyl *t*-butylthiosulphinate in β-cyclodextrin', Supramolecular Chemistry, 21: 7, 611 — 617
To link to this Article: DOI: 10.1080/10610270802613570
URL: http://dx.doi.org/10.1080/10610270802613570

Supramolecular Chemistry
Vol. 21, No. 7, October–November 2009, 611–617

Taylor & Francis
Taylor & Francis Group

Inclusion of the allicin mimic *S*-*p*-tolyl *t*-butylthiosulphinate in β-cyclodextrin

Nashia Stellenboom, Roger Hunter, Mino R. Caira*, Susan A. Bourne and Marco Barbieri

Department of Chemistry, University of Cape Town, Rondebosch, South Africa

(*Received 19 September 2008; final version received 4 November 2008*)

Allicin, the active thiosulphinate present in freshly crushed garlic, has potent antimicrobial activity but is chemically labile. As part of a study aimed at producing stable allicin analogues as potential antimicrobial agents, the allicin mimic *S*-*p*-tolyl *t*-butylthiosulphinate was synthesised and complexed with β-cyclodextrin (β-CD). The inclusion complex, β-CD·*S*-*p*-tolyl *t*-butylthiosulphinate·12.5H_2O, was characterised by thermal analysis techniques (HSM, TG, DSC), powder X-ray diffraction and single-crystal X-ray diffraction. The inclusion complex is dimeric (space group $C222_1$) with the guest disordered over three positions. Within each β-CD molecule of the dimer, each disordered guest component is located in the host cavity with the *t*-butyl group protruding slightly from the primary hydroxyl side, while the phenyl ring is situated near the secondary hydroxyl side and the thiosulphinate moiety is centrally located within the host cavity. Stereoselectivity of guest inclusion is implicit in the disordered model, which reflects a 2:1 ratio of *S*- and *R*-enantiomers in the β-CD cavity.

Keywords: thiosulphinate; allicin; cyclodextrin; X-ray diffraction; thermal analysis

Introduction

Allicin [*S*-(2-propenyl)-2-propene-1-sulphinothionate] (Figure 1) is a member of a class of unstable and reactive organosulphur compounds known as thiosulphinates and is the principal biologically active substance in freshly crushed garlic. Allicin is produced upon destroying the compartment that separates alliin and the enzyme alliinase, resulting in the two coming into close contact. A rapid elimination reaction ensues producing 2-propene-sulphenic acid, which self-condenses to produce the thiosulphinate allicin that accounts for about 70–80% of the organic material produced initially (*1*). In 1944, Cavallito and Bailey reported the isolation and identification of allicin and in 1947, Cavallito *et al*. established its chemical structure (*2*, *3*). They also demonstrated that the synthetic material obtained from selectively oxidising diallyl disulphide using perbenzoic acid was identical with that isolated from freshly crushed garlic (*3*).

Allicin has a pungent garlic odour, is extremely unstable in neat form, is moderately volatile and poorly miscible in aqueous solutions. Its instability depends on a range of parameters including pH, concentration, temperature, solvent and the presence of additives that can cause its rapid transformation into a variety of secondary compounds (*4*). However, allicin possesses a range of potent biological activities, including antimicrobial (antibacterial, antifungal, antiviral and antiparasitic), antioxidant, antitumour, antithrombotic and antiatherosclerotic (*2*, *5–8*). In addition, allicin acts as a systematic vasodilator with an antihypertensive effect, inhibits platelet aggregation, inhibits alcohol dehydrogenase and inactivates various cysteine proteinases (*9–11*).

A literature survey revealed that certain saturated thiosulphinates are both more active and more stable than allicin. In the light of this and our earlier study of the inclusion of one of the allicin's transformation products, ajoene, in heptakis(2,3,6-tri-*O*-methyl)-β-cyclodextrin (TRIMEB) (*12*), our interest now focuses on the possible inclusion of allicin mimics in cyclodextrins (CDs). The term 'mimic' in this context refers to a structural analogue with a biological profile likely to be similar to allicin. Practical advantages to be gained by CD inclusion of the allicin mimics generally are enhancement of their stability, masking of their offensive odours, improvement in their aqueous solubility and (in the case of mimics that are liquid at room temperature) their conversion into solid complexes.

In this report, we describe the preparation of the inclusion complex formed between the allicin mimic *S*-*p*-tolyl *t*-butylthiosulphinate (Figure 1) and β-CD by both kneading and co-precipitation methods, as well as complex characterisation by thermal analysis, powder X-ray diffraction (PXRD) and single-crystal X-ray diffraction (XRD). The latter technique revealed a very unusual structural feature, namely three-fold disorder of the included guest molecule. Furthermore, owing to the tetrahedral geometry around the sulphinyl S atom of the guest molecule, this centre is rendered chiral and structural elucidation of the complex therefore also

*Corresponding author. Email: mino.caira@uct.ac.za

ISSN 1061-0278 print/ISSN 1029-0478 online

DOI: 10.1080/10610270802613570
http://www.informaworld.com

Figure 1. Chemical structures of allicin (left) and *S-p*-tolyl *t*-butylthiosulphinate (right).

involved establishment of the extent of stereoselective guest inclusion.

Experimental

Complex preparation and preliminary characterisation

β-CD was purchased from Cyclolab (Budapest, Hungary) and *S-p*-tolyl *t*-butylthiosulphinate was synthesised via *meta*-chloroperbenzoic acid (*m*-CPBA) oxidation of the corresponding unsymmetrical disulphide prepared using methodology recently described by Hunter *et al*. (*13*) (Scheme 1). An alternative synthesis was reported earlier (*14*). As an initial test for complex formation, equimolar amounts of host and guest were kneaded for 1 h with continual addition of small amounts of distilled water. The resultant material was characterised by PXRD (see below). For the preparation of single crystals of the complex, β-CD (49 mg, 0.04 mmol) was dissolved in 4 ml distilled water at 65°C. An equimolar amount of *S-p*-tolyl *t*-butylthiosulphinate (10 mg, 0.04 mmol) was added to the solution followed by vigorous stirring for 4 h. The solution was filtered (0.45 μm) and left at room temperature to induce crystallisation. Several crystals of the complex were removed from the mother liquor and surface-dried on filter paper for thermal analysis.

Hot-stage microscopy (HSM) was used to study the morphological and physical changes of the complex crystals as they were slowly heated over the temperature range 0–300°C. Crystals were immersed in silicone oil between two glass coverslips and placed on a Linkam THMS600 hot stage apparatus mounted on a Nikon SMZ-10 stereoscopic microscope fitted with a Linkam TP92 temperature controller. Images were captured using a real-time Sony Digital Hyper HAD colour video camera and viewed and analysed using the Soft Imaging System program analysis (*15*).

Thermogravimetry (TGA) was performed on a Perkin-Elmer PC7-Series instrument at a scanning rate of $10\,K\,min^{-1}$ under N_2 gas at a flow rate of $30\,cm^3\,min^{-1}$ to determine complex thermal stability as well as crystal water content. Differential scanning calorimetry (DSC) was carried out on a Perkin-Elmer DSC7 instrument under N_2 gas at a flow rate of $30\,cm^3\,min^{-1}$ and a scanning rate of $10\,K\,min^{-1}$. Samples (4–7 mg range) were placed in vented aluminium pans and scanned over the range 30–300°C.

Host–guest stoichiometry was determined as 1:1 from proton integration ratios extracted from the ^1H NMR spectrum (Varian Mercury, 300 MHz) of a solution of complex single crystals in CD_3Cl. Integration of the guest *t*-butyl proton peaks (δ 1.73 ppm) and host H6 peaks (δ 4.10 ppm) yielded a ratio of 9:14.2 (calculated 9:14 for 1:1 host–guest stoichiometry). Other host–guest proton ratios were consistent with this estimate.

Powder X-ray diffraction

The product of kneading β-CD and *S-p*-tolyl *t*-butylthiosulphinate was spread uniformly on Mylar® film. Powder obtained by gentle manual grinding of single crystals was loaded into a Lindemann capillary. XRD data were collected on a Huber Imaging Plate Guinier Camera 670 employing Ni-filtered Cu $K\alpha_1$ radiation ($\lambda = 1.5406$ Å) produced at 40 kV and 20 mA by a Philips PW1120/00 generator. Accessories included a Huber long fine-focus tube PW2273/20 and a Huber Guinier Monochromator Series 611/15. Multiscans over 10–60 min were employed over the 2θ range 0–30°.

Single crystal X-ray analysis

An equant crystal fragment of the inclusion complex (hereafter **1**) was cut from a larger crystal, coated with paratone N oil (Exxon) and mounted on a Nonius Kappa CCD Single Crystal X-ray Diffractometer using graphite-monochromated Mo Kα radiation ($\lambda = 0.71069$ Å). The specimen was bathed in a constant stream of nitrogen vapour maintained at 113(2) K by an Oxford Cryostream cooler (Oxford Cryosystems, Witney, UK). It was established that cooling the crystal from 291 to 113 K did not induce any phase changes.

Data collection (COLLECT software (*16*)) involved a combination of ϕ- and ω-scans of 0.8–1.0° and a crystal to detector distance in the range 45.0–47.0 mm. All data were corrected for Lorentz-polarisation effects. Unit cell refinement and data reduction were performed using DENZO-SMN and SCALEPACK (*17*). The orthorhombic crystal system was established from the Laue symmetry

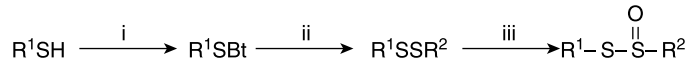

Scheme 1. Synthesis of *S-p*-tolyl *t*-butylthiosulphinate. Reagents and conditions: (i) BtCl (1.5 equiv.), BtH (1 equiv.), CH_2Cl_2, −78°C, 2 h. (ii) R^2SH (1.5 equiv.), CH_2Cl_2, −20°C, 30 min. (iii) *m*-CPBA, CH_2Cl_2, −78°C, rt. (R^1SH = *p*-tolylthiol and R^2SH = *t*-butylthiol.)

(*mmm*) and the space group $C222_1$ from systematic absences.

The phase problem was solved using a trial model based on the atomic co-ordinates of the rigid part of the β-CD molecule in the isostructural complex containing the guest 4-*t*-butylbenzyl alcohol (*18*). Remaining non-H atoms in the single host molecule of the asymmetric unit were located in difference Fourier maps. Of these, two primary hydroxyl oxygen atoms (O6G1 and O6G5) were disordered over two positions and were modelled accordingly. Except for these, all non-H atoms of the host refined anisotropically. Following refinement of the host molecule and addition of H atoms in idealised positions in a riding model (*19*), the residual difference Fourier electron density peaks were abnormally low, but distinct images of the three disordered guest components emerged. Modelling of the disorder was tedious, requiring many cycles of least-squares refinement for convergence. All guest atoms were modelled by assigning the three disordered components (A, B and C), a common U_{iso} parameter (final refined value 0.081 Å^2) and individual site-occupancy factors (SOFs) which initially refined freely to 0.28, 0.33 and 0.34 for components A, B and C, respectively. Given the low electron densities involved, the symmetry of the emerging disordered guest arrangement and the 1:1 stoichiometry indicated by the ^{1}H NMR data, these SOF values were deemed sufficiently close to 1/3 each to justify constraining them as such in the final cycles of refinement. Only one guest atom (a sulphoxide oxygen, O1BC) shared a common site in disordered components B and C and was assigned an SOF of 2/3. Guest phenyl rings were constrained as regular hexagons and several distance restraints ($\sigma = 0.01$ Å) were employed to ensure reasonable guest geometries. As for the host, guest H atoms were added in idealised positions in a riding model with U_{iso} in the range 1.2–1.5 times those of their parent atoms.

Ten oxygen atoms corresponding to water molecules were initially located and assigned full site occupancies. An additional five sites for water oxygen atoms were found and their SOFs refined, while their U_{iso} values were set to the mean of those of the ordered oxygen atoms. The sum of the SOFs was 12.46, in accord with the value of 12.5 water molecules estimated by TGA (see below). H atoms of the water molecules were not located.

Details of the crystal parameters, data collection and refinement of the structure are listed in Table 1. Crystallographic data (excluding structure factors) for complex **1** have been deposited with the Cambridge Crystallographic Data Centre, as CCDC No. 699654. Copies of the data can be obtained free of charge on application to CCDC, 12 Union Road, Cambridge CB2 1EZ, UK (fax: +44 1223-336-033; e-mail: deposit@ccdc.cam.ac.uk).

Results and discussion

PXRD analysis

To detect inclusion complex formation, the experimental PXRD pattern of the material obtained by kneading β-CD and *S*-*p*-tolyl *t*-butylthiosulphinate (Figure 2, centre) was compared with computed PXRD patterns for both crystalline β-CD hydrate and various series of isostructural β-CD inclusion complexes (*20*). No match was obtained with the

Table 1. Crystallographic data for complex **1**.

Formula	$C_{42}H_{70}O_{35}{\cdot}C_{11}H_{16}OS_2{\cdot}12.5H_2O$
Formula weight	1588.54
Temperature (K)	113(2)
Crystal system	Orthorhombic
Space group	$C222_1$
a (Å)	19.1873(1)
b (Å)	23.9921(2)
c (Å)	32.4473(3)
Volume (Å^3)	14,936.9(2)
Z	8
Density (calc.) (g cm^{-3})	1.413
Radiation, wavelength (Å)	Mo Kα, 0.71073
Absorption coefficient (mm^{-1})	0.178
F(000)	6792
Crystal size (mm^3)	0.32 × 0.26 × 0.22
Theta range (°)	1.0–25.35
Index ranges	$-23 \le h \le 21$; $-28 \le k \le 28$; $-39 \le l \le 39$
Reflections collected/unique	71,011/13,662
Observed reflections [$I > 2\sigma(I)$]	11,621
Data/restraints/parameters	13,662/24/874
Goodness-of-fit on F^2	1.043
Final *R*-indices R_1, wR^2 [$I > 2\sigma(I)$]	0.0903/0.2531
R-indices R_1, wR^2 (all data)	0.1021/0.2670
Largest diff. peak and hole (eÅ^{-3})	−0.83 and 1.19

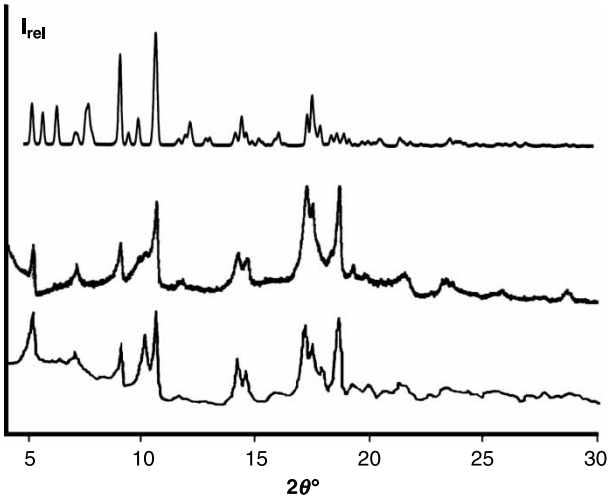

Figure 2. Reference PXRD pattern no. 13 (top), experimental pattern of the material obtained by kneading the host and guest (centre) and experimental pattern of the complex **1** obtained by co-precipitation (bottom).

pattern for the uncomplexed host. Figure 2 (top) shows the pattern which matches most closely, namely that of the reference PXRD pattern for isostructural series no. 13 (orthorhombic β-CD complexes crystallising in the space group $C222_1$ with $a \sim 19.2$, $b \sim 23.9$, $c \sim 32.4$ Å with the complex units packing in the 'chessboard' motif (*18*)). As explained earlier (*20*), the level of correspondence indicated in Figure 2 is sufficient evidence for deducing inclusion complex formation as well as the crystal parameters quoted. The PXRD pattern of ground single crystals of complex **1** obtained by co-precipitation (Figure 2, bottom) is in very good agreement with that for the product of kneading, confirming that both methods produce the same inclusion complex. Single crystal XRD (see below) confirmed the space group and unit cell dimensions predicted from PXRD.

Thermal analysis

The combined TGA and DSC traces for complex **1** are shown in Figure 3. In the temperature range 30–170°C, the trace shows a mass loss of 14.3% (event **A**) which

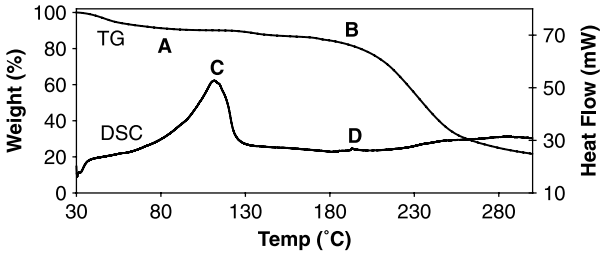

Figure 3. TGA and DSC traces for complex **1**.

is equivalent to 12.5 water molecules per complex unit. It is somewhat unusual for water molecules to be retained up to temperatures as high as those indicated and for them to be lost in a two-step process, the second mass loss commencing at ~120°C. This behaviour is attributed to strong interactions the water molecules experience within the CD complex packing arrangement, as indicated from the crystal structure. Consistent with HSM analysis, the complex decomposes at an onset temperature of 185°C represented by **B**. In agreement with the HSM and TGA experiments, a broad endotherm (**C**) with a peak at 112°C was observed in the DSC, due to dehydration. This was followed by decomposition of the anhydrous complex at ~185°C (broad endotherm commencing at **D**).

Single-crystal X-ray analysis

The crystallographic asymmetric unit in complex **1** comprises one β-CD molecule, one *S*-*p*-tolyl *t*-butylthiosulphinate molecule and 12.5 water molecules. Two asymmetric units form a dimer with two-fold crystallographic symmetry. In the host molecule, all glucose residues adopt the usual $^4C_1$ conformation. Two of the primary hydroxyl oxygen atoms (glucose residues G1 and G5) are disordered over two positions. All primary hydroxyl groups are directed away from the cavity in a (−)-*g* [(−)-*gauche*] conformation except in residues G1 and G5, where both (+)-*g* and (−)-*g* conformations are manifested by the disorder. Molecular parameters for the host and their respective ranges are as follows: glycosidic oxygen angles O4G(n)···O4G($n-1$)···O4G($n-2$) (126.3–130.3°), O4···O4′ distances (4.31–4.40 Å), radii of the O4-heptagon (4.97–5.10 Å), tilt angles (3.3–11.7°), intra-glucose O2···O3′ distances (2.72–2.84 Å) and deviations of the seven O4 atoms from the mean O4-plane (−0.022(2) to +0.028(2) Å). These data indicate that guest inclusion does not cause significant distortion of the host molecule.

Of primary interest here is the mode of guest inclusion in the host cavity and the unusual nature of the guest disorder. Figure 4 shows the composite guest model A–B–C based on interpretation of the observed electron density in the host cavity. This image represents the overlapping triplet of disordered guest components, while the figures labelled A, B and C represent the deconvoluted components. Three features are highlighted here, namely the approximate three-fold symmetry of the image A–B–C, the common position occupied by the sulphoxide oxygen atom O1 in disordered components B and C (O1BC), and the configurations at the stereogenic centres. The latter (*S*-, *S*-, *R*-) indicate that for the crystal analysed, some degree of stereoselectivity accompanies guest inclusion under the preparative conditions employed.

Refined values of unconstrained molecular parameters (bond lengths, bond angles) in the three disordered guest components are in the expected ranges. The orientation

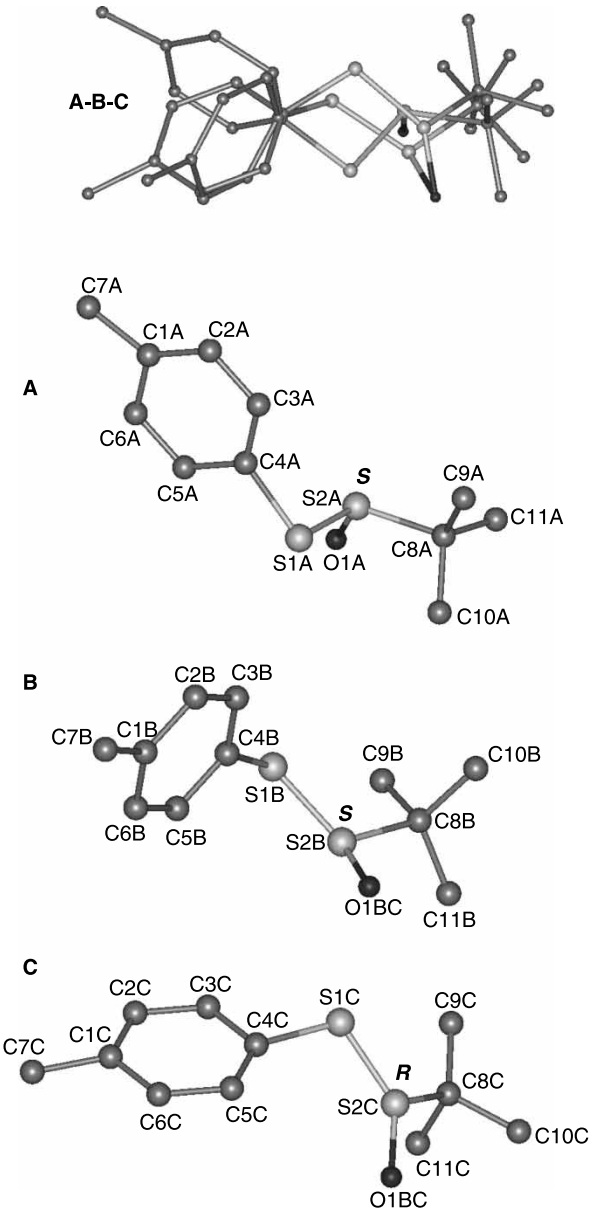

Figure 4. Composite electron density of guest peaks within the β-CD cavity (A–B–C) and the individual components of disorder A, B and C.

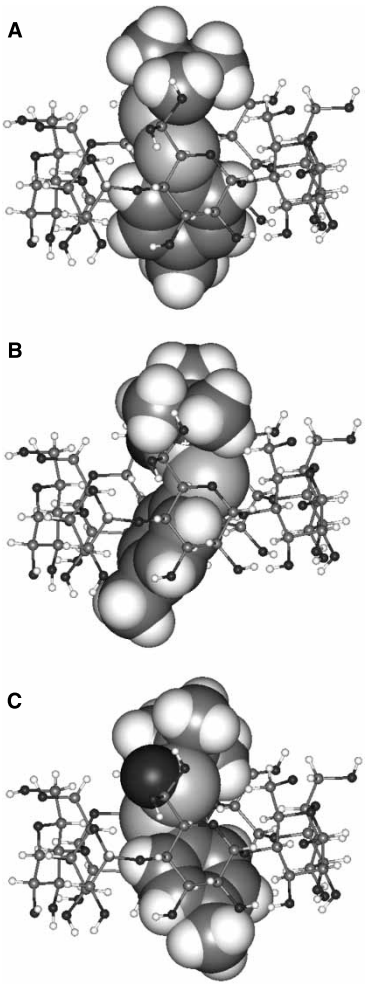

Figure 5. Analogous modes of inclusion of the disordered guest components in the β-CD cavity.

of the *p*-tolyl residue with respect to the thiosulphinate group varies considerably. This is described by a common torsion angle C_{ar}–C_{ar}–S–S which has values −88(1)° (A), 106(1)° (B) and −140(1)° (C). The *t*-butyl group is staggered relative to the S═O bond in each disordered component.

Figure 5 shows separately the common mode of inclusion of each disordered component within the same β-CD cavity. In all cases, the *t*-butyl group protrudes from the primary side, consistent with the majority of the C6–O6 primary hydroxyl groups being rotated away from the centre of the CD cavity, where they can hydrogen bond with water molecules and/or other host molecules. The guest methyl groups protrude from the host secondary side, partially occupying the cavity of the second β-CD molecule comprising the dimeric complex. Location of the guest methyl groups at the dimer interface is evident in the cutaway view of Figure 6, where for clarity only one guest component (A) and its diad-related partner have been included in the figure. For the three pairs of diad-related disordered guest molecules, the distances between the centroids of the phenyl rings are 4.78 Å (A···A), 4.57 Å (B···B) and 4.51 Å (C···C). Inclusion of the allicin mimic is based exclusively on hydrophobic interactions between the host and guest molecules. The lack of distinct, directional host–guest interactions is thus consistent with the orientational guest disorder observed.

The crystal structure of the inclusion complex is maintained by a complex network of O–H···O hydrogen

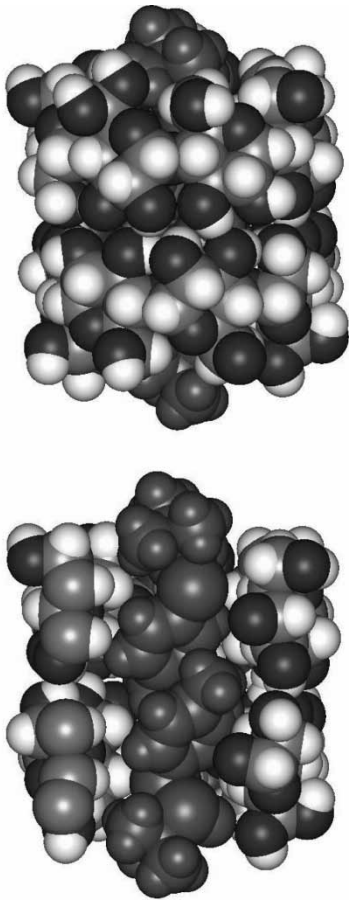

Figure 6. Space-filling view of the dimeric complex (top) and a cutaway view (bottom) illustrating inclusion of a representative guest disorder component.

bonds, including six intra-dimer H-bonds that involve the host secondary hydroxyl groups, nine H-bonds between host hydroxyl groups and water molecules, and ~25 between water molecules. Crystal packing conforms to the well-known 'chessboard' arrangement, described earlier (*18*).

Concluding remarks

In a recent study, we described the X-ray structure of the monomeric 1:1 inclusion complex of the allicin mimic *S-p*-methoxyphenyl propylthiosulphinate with the host permethylated β-CD (TRIMEB) (*21*). Closure of the primary side of the host molecule by methoxyl groups resulted in the guest molecule adopting a hairpin conformation, with both termini located near the host secondary face. The present study reports the first instance of structural elucidation of an allicin mimic in the native host β-CD. In this case, the complex is dimeric, one end of the guest molecule protruding from the primary face of each host molecule comprising the dimer, while the other end is located at its secondary side. In addition, an unprecedented pseudo-three-fold guest disorder with a 2:1 *S-*/*R*-enantiomeric composition was detected and successfully modelled.

As allicin mimics represent a novel class of potentially useful antibacterials with proven pharmacological activity (*21*) but generally poor aqueous solubility, their inclusion in CDs has merit as a strategy for improving their delivery properties. Inclusion in native CDs, as exemplified by the present study, is more relevant in this context given their significantly lower cost and toxicity compared with their methylated counterparts. In this connection, unequivocal evidence based on PXRD analysis also indicated that kneading both *S-p*-methoxyphenyl propylthiosulphinate and *S-p*-tolyl *t*-butylthiosulphinate with γ-CD yields inclusion complexes whose PXRD patterns closely match that for the well-known tetragonal complex phase (space group $P4_12$) with approximate unit cell dimensions: $a \sim 23.8$ Å, $c \sim 23.2$ Å (*20*, *22*).

Acknowledgements

We thank the University of Cape Town and the NRF for financial assistance. This material is based on the work supported by the National Research Foundation under Grant number NRF 67941. Any opinions, findings and conclusions or recommendations expressed in the material are those of the author and do not necessarily reflect the views of the National Research Foundation.

References

(1) Ankri, S.; Mirelman, D. *Microbes Infect.* **1999**, *2*, 125–129.
(2) Cavallito, C.J.; Bailey, J.H. *J. Am. Chem. Soc.* **1944**, *66*, 1950–1951.
(3) Small, L.V.D.; Bailey, J.; Cavallito, C.J. *J. Am. Chem. Soc.* **1947**, *69*, 1710–1713.
(4) Freeman, F.; Kodera, Y. *J. Agric. Food Chem.* **1995**, *43*, 2332–2338.
(5) Harris, J.C.; Cottrell, S.L.; Plummer, S.; Lloyd, D. *Appl. Microbiol. Biotechnol.* **2001**, *57*, 282–286.
(6) Weber, N.D.; Andersen, D.O.; North, J.A.; Murray, B.K.; Lawson, L.D.; Hughes, B.G. *Planta Med.* **1992**, *58*, 417–423.
(7) Soffar, S.A.; Mokhtar, G.M. *J. Egypt. Soc. Parasitol.* **1991**, *21*, 497–502.
(8) Weisberger, A.S.; Pensky, J. *Cancer Res.* **1958**, *18*, 1301–1308.
(9) Elkayam, A.; Mirelman, D.; Peleg, E.; Wilchek, M.; Miron, T.; Rabinkov, A.; Sadetzki, S.; Rosenthal, T. *Am. J. Hypertens.* **2001**, *14*, 377–381.
(10) Briggs, W.H.; Xiao, H.; Parkin, K.L.; Shen, C.; Goldman, I.L. *J. Agric. Food Chem.* **2000**, *48*, 5731–5735.
(11) Rabinkov, A.; Miron, T.; Konstantinovski, L.; Wilchek, M.; Mirelman, D.; Weiner, L. *Biochem. Biophys. Acta* **1998**, *1379*, 233–244.
(12) Caira, M.R.; Hunter, R.; Bourne, S.A.; Smith, V.J. *Supramol. Chem.* **2004**, *16*, 395–403.
(13) Hunter, R.; Caira, M.R.; Stellenboom, N. *J. Org. Chem.* **2006**, *71*, 8268–8271.
(14) Colonna, S.; Pironti, V.; Drabowicz, J.; Brebion, F.; Fensterbank, K.; Malacria, M. *Eur. J. Org. Chem.* **2005**, *9*, 1727–1730.
(15) Analysis®, Soft Imaging System GmbH, *Digital Solutions for Imaging and Microscopy*, Version 3.1 for Windows © 1987–2000.

(16) Hooft, R. *COLLECT*, Nonius, B.V., Delft, The Netherlands, 1998.
(17) Otwinowski, Z.; Minor, W. In *Methods in Enzymology*; Carter, C.W., Sweet, R.M., Eds.; Academic Press: New York, 1997; Vol. 276, pp 307–326.
(18) Mentzafos, D.; Mavridis, I.M.; Le Bas, G.; Tsoucaris, G. *Acta Crystallogr., Sect. B: Struct. Sci.* **1991**, *B47*, 746–757.
(19) Sheldrick, G.M. *SHELXL-97*; University of Göttingen: Germany, 1997.
(20) Caira, M.R. *Rev. Roum. Chim.* **2001**, *46*, 371–386.
(21) Stellenboom, N.; Hunter, R.; Caira, M.R.; Bourne, S.A.; Cele, K.; Qwebani, T.; le Roex, T. *ARKIVOC* **2007**, *ix*, 53–63.
(22) Stellenboom, N. PhD Thesis, University of Cape Town, 2008, 202 pp.